ICHEP94 Ref. GLS0394 CLEO CONF 94-12
Submitted to PA 16,2 Pl 9,19 July 17, 1994

The Inclusive Decay $B \to \eta X$

R. Ammar,[1] P. Baringer,[1] A. Bean,[1] D. Besson,[1] D. Coppage,[1] N. Copty,[1] R. Davis,[1] N. Hancock,[1] M. Kelly,[1] S. Kotov,[1] I. Kravchenko,[1] N. Kwak,[1] H. Lam,[1] Y. Kubota,[2] M. Lattery,[2] M. Momayezi,[2] J.K. Nelson,[2] S. Patton,[2] R. Poling,[2] V. Savinov,[2] S. Schrenk,[2] R. Wang,[2] M.S. Alam,[3] I.J. Kim,[3] Z. Ling,[3] A.H. Mahmood,[3] J.J. O'Neill,[3] H. Severini,[3] C.R. Sun,[3] F. Wappler,[3] G. Crawford,[4] C. M. Daubenmier,[4] R. Fulton,[4] D. Fujino,[4] K.K. Gan,[4] K. Honscheid,[4] H. Kagan,[4] R. Kass,[4] J. Lee,[4] R. Malchow,[4] M. Sung,[4] C. White,[4] M.M. Zoeller,[4] F. Butler,[5] X. Fu,[5] B. Nemati,[5] W.R. Ross,[5] P. Skubic,[5] M. Wood,[5] M. Bishai,[6] J. Fast,[6] E. Gerndt,[6] R.L. McIlwain,[6] T. Miao,[6] D.H. Miller,[6] M. Modesitt,[6] D. Payne,[6] E.I. Shibata,[6] I.P.J. Shipsey,[6] P.N. Wang,[6] M. Battle,[7] J. Ernst,[7] L. Gibbons,[7] Y. Kwon,[7] S. Roberts,[7] E.H. Thorndike,[7] C.H. Wang,[7] J. Dominick,[8] M. Lambrecht,[8] S. Sanghera,[8] V. Shelkov,[8] T. Skwarnicki,[8] R. Stroynowski,[8] I. Volobouev,[8] G. Wei,[8] P. Zadorozhny,[8] M. Artuso,[9] M. Gao,[9] M. Goldberg,[9] D. He,[9] N. Horwitz,[9] G.C. Moneti,[9] R. Mountain,[9] F. Muheim,[9] Y. Mukhin,[9] S. Playfer,[9] Y. Rozen,[9] S. Stone,[9] X. Xing,[9] G. Zhu,[9] J. Bartelt,[10] S.E. Csorna,[10] Z. Egyed,[10] V. Jain,[10] D. Gibaut,[11] K. Kinoshita,[11] P. Pomianowski,[11] B. Barish,[12] M. Chadha,[12] S. Chan,[12] D.F. Cowen,[12] G. Eigen,[12] J.S. Miller,[12] C. O'Grady,[12] J. Urheim,[12] A.J. Weinstein,[12] M. Athanas,[13] W. Brower,[13] G. Masek,[13] H.P. Paar,[13] J. Gronberg,[14] R. Kutschke,[14] S. Menary,[14] R.J. Morrison,[14] S. Nakanishi,[14] H.N. Nelson,[14] T.K. Nelson,[14] C. Qiao,[14] J.D. Richman,[14] A. Ryd,[14] D. Sperka,[14] H. Tajima,[14] M.S. Witherell,[14] R. Balest,[15] K. Cho,[15] W.T. Ford,[15] D.R. Johnson,[15] K. Lingel,[15] M. Lohner,[15] P. Rankin,[15] J.G. Smith,[15] J.P. Alexander,[16] C. Bebek,[16] K. Berkelman,[16] K. Bloom,[16] T.E. Browder,[16*] D.G. Cassel,[16] H.A. Cho,[16] D.M. Coffman,[16] D.S. Crowcroft,[16] P.S. Drell,[16] D. Dumas,[16] R. Ehrlich,[16] P. Gaidarev,[16] M. Garcia-Sciveres,[16] B. Geiser,[16] B. Gittelman,[16] S.W. Gray,[16] D.L. Hartill,[16] B.K. Heltsley,[16] S. Henderson,[16] C.D. Jones,[16] S.L. Jones,[16] J. Kandaswamy,[16] N. Katayama,[16] P.C. Kim,[16] D.L. Kreinick,[16] G.S. Ludwig,[16] J. Masui,[16] J. Mevissen,[16] N.B. Mistry,[16] C.R. Ng,[16] E. Nordberg,[16] J.R. Patterson,[16] D. Peterson,[16] D. Riley,[16] S. Salman,[16] M. Sapper,[16] F. Würthwein,[16] P. Avery,[17] A. Freyberger,[17] J. Rodriguez,[17] S. Yang,[17] J. Yelton,[17] D. Cinabro,[18] T. Liu,[18] M. Saulnier,[18] R. Wilson,[18] H. Yamamoto,[18] T. Bergfeld,[19] B.I. Eisenstein,[19] G. Gollin,[19] B. Ong,[19] M. Palmer,[19] M. Selen,[19] J. J. Thaler,[19] K.W. Edwards,[20] M. Ogg,[20] A. Bellerive,[21] D.I. Britton,[21] E.R.F. Hyatt,[21] D.B. MacFarlane,[21] P.M. Patel,[21] B. Spaan,[21] and A.J. Sadoff[22]

(CLEO Collaboration)

[1] *University of Kansas, Lawrence, Kansas 66045*
[2] *University of Minnesota, Minneapolis, Minnesota 55455*
[3] *State University of New York at Albany, Albany, New York 12222*
[4] *Ohio State University, Columbus, Ohio, 43210*
[5] *University of Oklahoma, Norman, Oklahoma 73019*
[6] *Purdue University, West Lafayette, Indiana 47907*
[7] *University of Rochester, Rochester, New York 14627*
[8] *Southern Methodist University, Dallas, Texas 75275*
[9] *Syracuse University, Syracuse, New York 13244*
[10] *Vanderbilt University, Nashville, Tennessee 37235*
[11] *Virginia Polytechnic Institute and State University, Blacksburg, Virginia, 24061*
[12] *California Institute of Technology, Pasadena, California 91125*
[13] *University of California, San Diego, La Jolla, California 92093*
[14] *University of California, Santa Barbara, California 93106*
[15] *University of Colorado, Boulder, Colorado 80309-0390*
[16] *Cornell University, Ithaca, New York 14853*
[17] *University of Florida, Gainesville, Florida 32611*
[18] *Harvard University, Cambridge, Massachusetts 02138*
[19] *University of Illinois, Champaign-Urbana, Illinois, 61801*
[20] *Carleton University, Ottawa, Ontario K1S 5B6 and the Institute of Particle Physics, Canada*
[21] *McGill University, Montréal, Québec H3A 2T8 and the Institute of Particle Physics, Canada*
[22] *Ithaca College, Ithaca, New York 14850*

Abstract

Using data samples from the $\Upsilon(4S)$ resonance and nearby continuum taken with the CLEO II detector at CESR, we have measured the inclusive rate $\mathcal{B}(B \to \eta X)$=(17.6±1.1±1.2)%, and the momentum distribution of the η mesons using the $\eta \to \gamma\gamma$ decay mode.

*Permanent address: University of Hawaii at Manoa

The η meson is an interesting object. In the quark model it can be formed from an $s\overline{s}$ pair, or a "light" pair of either $d\overline{d}$ or $u\overline{u}$ quarks. This contrasts with the ϕ meson which is formed only from an $s\overline{s}$ pair. The inclusive B branching ratio to ϕ is $(2.3\pm0.8)\%$ [1]. In this paper we report a measurement of the branching ratio and momentum spectrum of η mesons from B decay, and estimate the fraction of η's that arise from fragmentation of the virtual W.

The data samples were taken by the CLEO II detector at the CESR e^+e^- collider [2]. A total luminosity on the peak of the $\Upsilon(4S)$ of 927 pb^{-1} and 416 pb^{-1} on the continuum was used. Hadronic events are selected by requiring at least 3 charged tracks originating from the interaction region and visible energy of at least 15% of the total center of mass energy. To suppress continuum background we require that the event shape parameter R2, the ratio of second and zeroth Fox Wolfram moments [3], be less than 0.3. In this analysis we detect photons only in the central region of the barrel portion of the calorimeter where $|\cos\theta| < 0.71$. The fractional γ energy resolution is $\delta E/E(\%) = 0.35/E^{3/4} + 1.9 - 0.1E$, ($E$ in GeV).

We measure the η yield in each 100 MeV interval in momentum on both the $\Upsilon(4S)$ and the continuum. The yield from B's is determined by subtracting the two distributions, properly accounting for relative luminosity and energies and then correcting for efficiencies. Since there is a large branching ratio for $\eta \to \gamma\gamma$ of 38.9% [4], and the CLEO II detector has excellent photon detection with its CsI crystal electromagnetic calorimeter, we use only this mode. We require that each photon candidate be found in a single isolated neutral energy cluster with minimum energy of 10 MeV, and with a lateral shower shape consistent with that expected for photons. The decay angle of the γ in the $\gamma\gamma$ center of mass is required to have a cosine less than 0.85 to eliminate combinatoric background which tends to preferentially populate asymmetric decays.

We use the sum of $\Upsilon(4S)$ and continuum data without a $R2$ cut to define the parameters for the signal function. These data can be fit well with an asymmetric-Gaussian signal function. The asymmetry comes from the loss of detected γ energy due to crystal rear end leakage. Fig. 1 shows the $\gamma\gamma$ mass spectrum for the sum of $\Upsilon(4S)$ and continuum data, for the momentum intervals (a) 0.8-0.9 GeV/c and (b) 1.4-1.5 GeV/c. The curves are fits to a polynomial background and an asymmetric Gaussian signal function whose parameters are allowed to vary.

We find that the mass is constant as a function of momentum with an average value of 547.0 ± 0.3 MeV, which is consistent with the new world average value 547.45 ± 0.19 Mev [4]. We fix the η mass in all fits to have this central value. The two r.m.s. widths, σ_A and σ_B, representing the lower mass and higher mass sides of the signal, respectively, have also been derived from the data. These are shown in Fig. 2 (a) and (b). The same r.m.s. widths obtained from Monte Carlo simulation are shown in Fig. 2 (c) and (d). In the low momentum region the data do not determine these widths well due to the large π^0 background. In contrast, the widths found from the Monte Carlo are poorly determined in the high momentum region above 2.0 Gev due to insufficient statistics. In the intermediate region the agreement between data and Monte Carlo is excellent. We have chosen to use the weighted average of the data and Monte Carlo distributions for the variation of these σ's with momentum. In Fig. 2 (e) and (f) we show this average and third order polynomial fits which we use to fix the σ's in our subsequent analysis.

In Fig. 3, the $\gamma\gamma$ invariant mass plot for the η momentum interval 0.8 to 2.0 GeV/c is shown for: (a) $\Upsilon(4S)$ data , (b) continuum data , and (c) $\Upsilon(4S)$ data after scaled continuum subtraction. The number of signal events is derived from (c). The number of events, the efficiency and the branching ratio in each momentum interval are listed in Table I . (The efficiency does not include the $\eta \to \gamma\gamma$ branching ratio.)

The efficiency, found by Monte Carlo simulation, is shown as a function of η momentum in Fig. 4 .

TABLE I. Numbers of Events

P (GeV)	# of events	ϵ(%)	$\mathcal{B}$(%/GeV)
0.0-0.1	500±189	39.5	1.7±0.6
0.1-0.2	810±416	34.2	3.1±1.6
0.2-0.3	2519±1092	30.2	11.1±4.8
0.3-0.4	4397±878	27.4	21.3±4.3
0.4-0.5	3207±986	25.5	16.7±5.1
0.5-0.6	3812±684	24.4	20.7±3.7
0.6-0.7	3581±579	23.9	19.9±3.2
0.7-0.8	3658±410	24.0	20.2±2.3
0.8-0.9	2534±339	24.4	13.8±1.8
0.9-1.0	2383±284	25.1	12.6±1.5
1.0-1.1	1672±219	26.0	8.5±1.1
1.1-1.2	1518±188	26.9	7.5±0.9
1.2-1.3	905±161	27.8	4.3±0.8
1.3-1.4	999±138	28.6	4.6± 0.6
1.4-1.5	589±122	29.4	2.7±0.6
1.5-1.6	486±105	30.0	2.2±0.5
1.6-1.7	407±94	30.4	1.8±0.4
1.7-1.8	250±82	30.7	1.1±0.4
1.8-1.9	240±73	30.8	1.0±0.3
1.9-2.0	50±66	30.8	0.2±0.3
2.0-2.1	169±57	30.6	0.7±0.2
2.1-2.2	78±51	30.1	0.3±0.2
2.2-2.3	45±48	30.1	0.2±0.2
2.3-2.4	-76±45	30.1	-0.3±0.2
2.4-2.5	86±39	30.1	0.4±0.2

The photon detection efficiency in the barrel calorimeter is about 50%, hence, the $\eta \to \gamma\gamma$ mode will have a reconstruction efficiency around 25% if the directions of the two γ's are uncorrelated. The efficiency increases at lower momentum, however, due to the nearly complete correlation in directions of the two γ's, and at higher momentum due to the partial correlation. We fit the efficiency curve to smooth the statistical fluctuations and then use the fitted values to deduce the rates. The resulting momentum spectrum is shown in Fig. 5. The errors shown are statistical only. The total branching ratio is obtained by summing the data from the individual momentum bins. We find $\mathcal{B}(B \to \eta X)$= (17.6±1.1±1.2)%. The major systematic error arises from the uncertainty in the η detection efficiency. This has been studied by measuring the ratio $\Gamma(\eta \to \pi^0\pi^0\pi^0)/\Gamma(\eta \to \gamma\gamma)$. We use an uncertainty of 6%. We estimate the overall systematic error from background parameterization to be 3%. We have found that the yield is insensitive to the value of the $R2$ cut which is used.

The η yield found here is about a factor of 7 larger than the ϕ yield. Several processes could yield a significant amount of η's. These include D^0 and D^+ decay, D_s decay, and fragmentation of the virtual W^-. We estimate the branching ratios for η production via D^0, D^+,and D_s decay by summing the branching ratios that have been observed to date [5]. The values are listed in Table II. We subtract the estimated branching ratio for these sources from our measured inclusive branching ratio to obtain our estimate of the for η's produced from the virtual W^-. The result is given in Table II.

A Monte Carlo calculation of the shapes of the momentum spectrum from each of the sources is shown in Fig. 6 (a), (b), and (c). The squares in Fig. 6 (d) represent the sum of (a), (b), and (c), with relative weights given by the partial branching ratios shown in Table II and normalized to the inclusive branching ratio. The triangles represent the data. The Monte Carlo predicts a softer spectrum than we observe.

TABLE II. Branching Ratio of the Three $B \to \eta X$ Processes

Process	Branching Ratio
$B \to D(D^0, D^+) \to \eta$	(2.5±0.5)% (from ref [5])
$B \to D_s \to \eta$	(2.8±0.6)% (from ref [5])
$B \to W^- \to \eta$	(12.3±1.8)% (Derived by subtraction)
Total	(17.6±1.6)%

In conclusion, we measure $\mathcal{B}(B \to \eta X)$=(17.6±1.1±1.2)%. This rate indicates that virtual W^- fragmentation is the dominant process in η production.

We gratefully acknowledge the effort of the CESR staff in providing us with excellent luminosity and running conditions. This work was supported by the National Science Foundation, the U.S. Dept. of Energy, the Heisenberg Foundation, the SSC Fellowship program of TNRLC, Natural Sciences and Engineering Research Council of Canada, and the A.P. Sloan Foundation.

REFERENCES

[1] D. Bortoletto et al., Phys. Rev. Lett. **56**, 800 (1986).
[2] CLEO Collaboration, Y. Kubota et al., Nucl. Inst. and Meth. **66**, A320 (1992).
[3] G. Fox and S. Wolfram, Phys. Rev. Lett. **41**, 1581 (1978).
[4] Particle Data Group, K. Hikasa *et al.*, Phys. Rev. D **45**, Part II (1992).
[5] Particle Data Group - 1994 preliminary draft

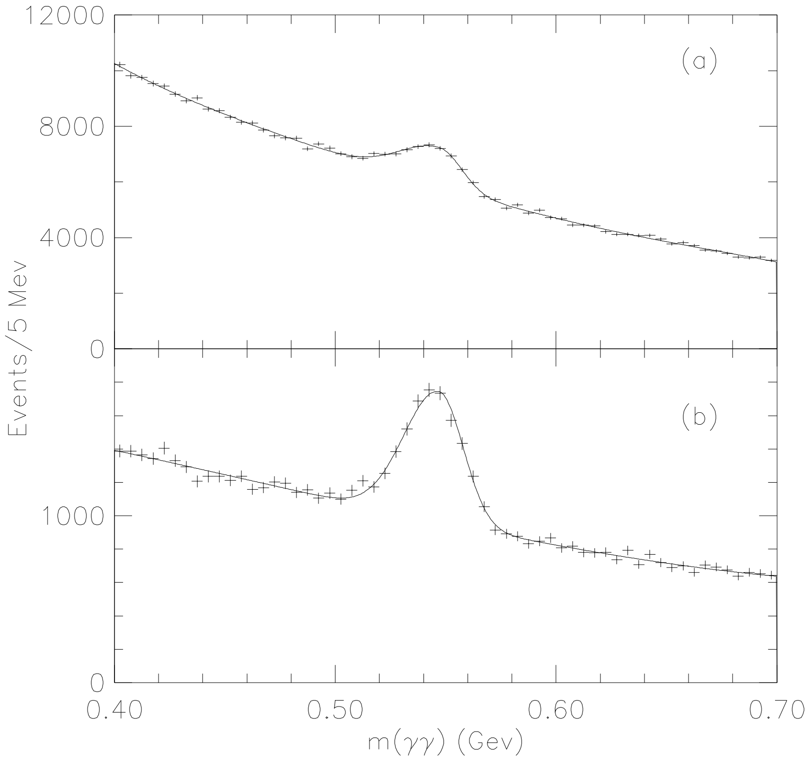

FIG. 1. The $\gamma\gamma$ mass spectrum for the sum of $\Upsilon(4S)$ and continuum data, for the momentum intervals (a) 0.8-0.9 GeV/c and (b) 1.4-1.5 GeV/c.

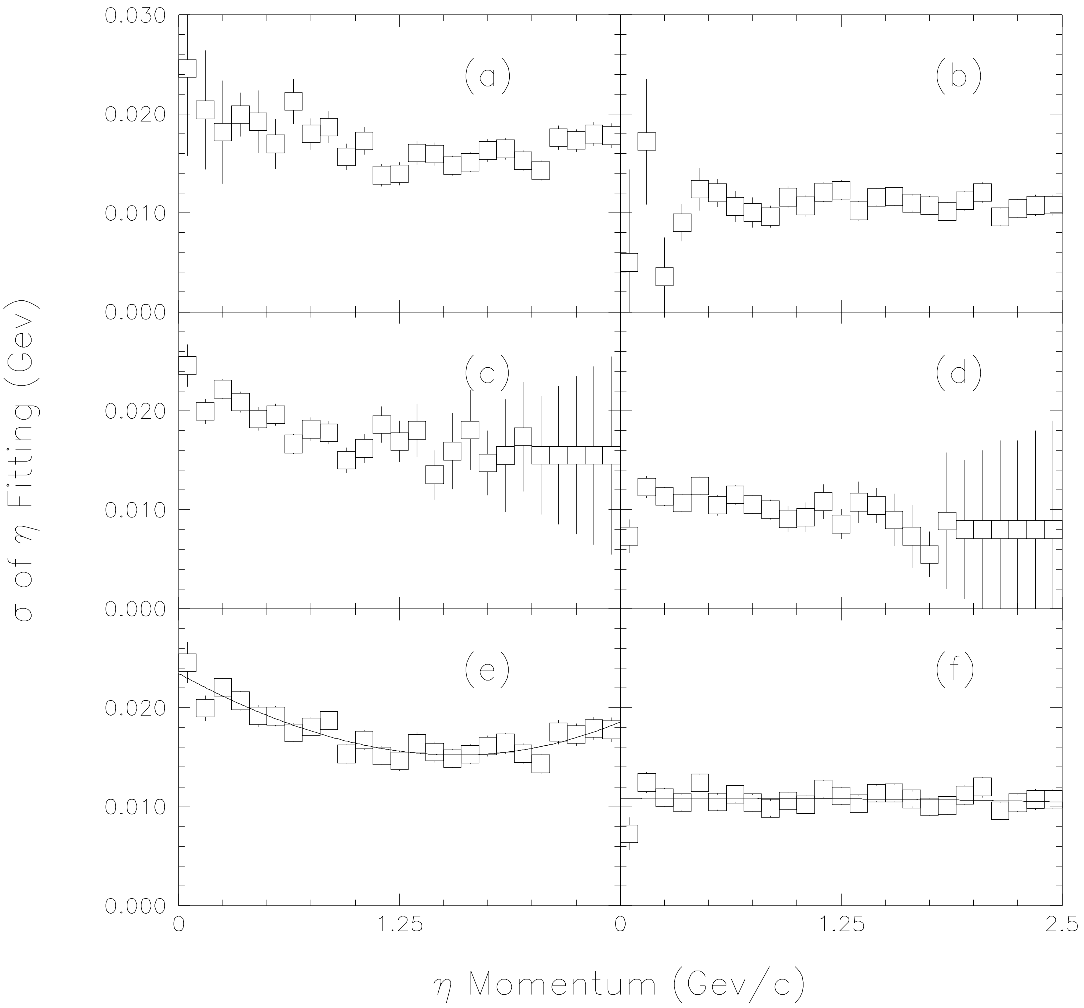

FIG. 2. σ_A and σ_B given as functions of η momenta as determined from data (a) and (b) and Monte Carlo simulation (c) and (d). In (e) and (f) the error weighted average of the data and Monte Carlo is shown with fits to third order polynomial.

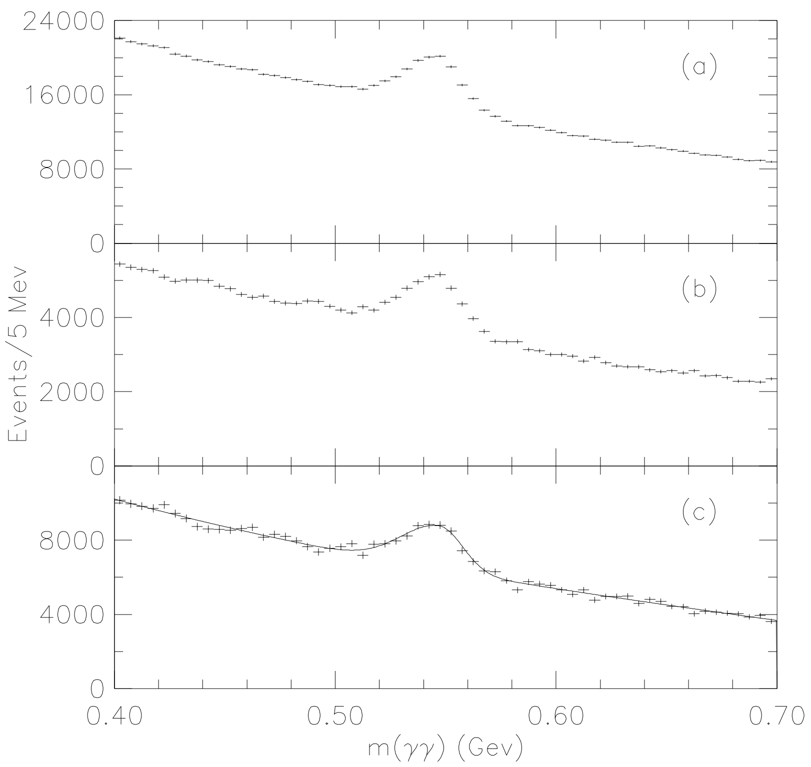

FIG. 3. The $\gamma\gamma$ mass spectrum for (a)$\Upsilon(4S)$ data, (b) continuum data, and (c) scaled continuum subtracted. The η momentum interval is 0.8 to 2.0 GeV/c.

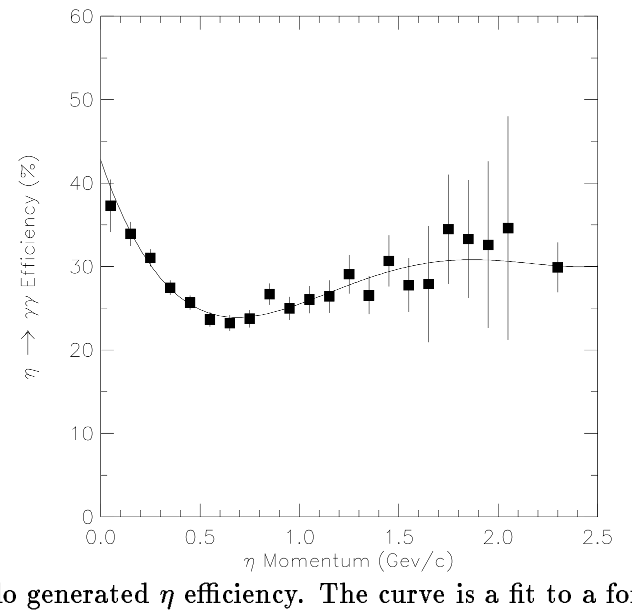

FIG. 4. Monte Carlo generated η efficiency. The curve is a fit to a forth order polynomial.

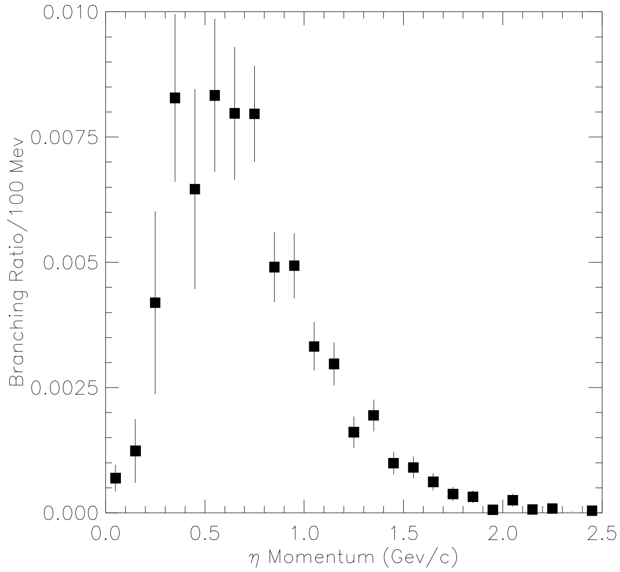

FIG. 5. Measured η momentum spectrum from B decay.

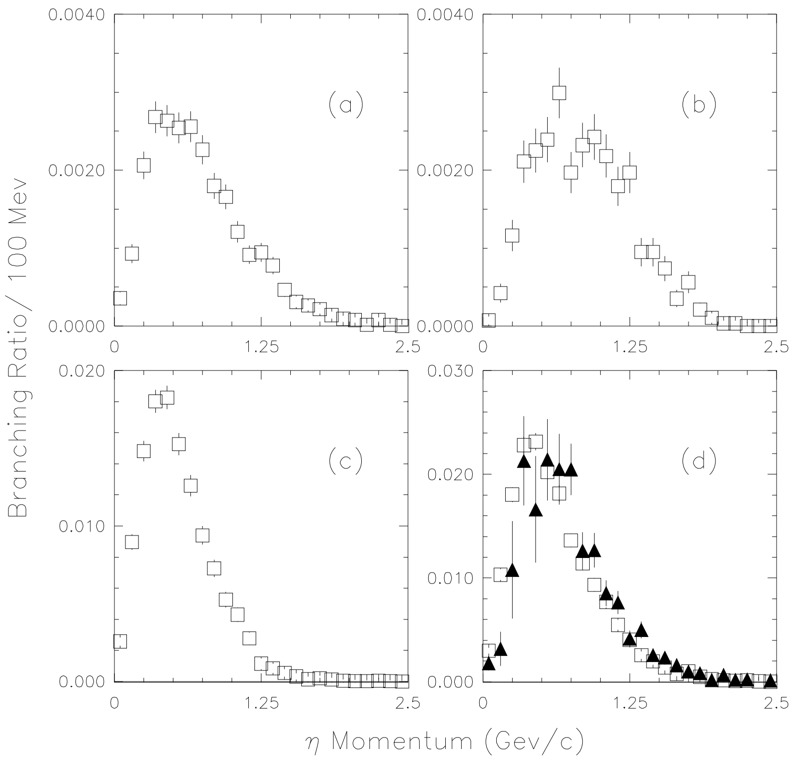

FIG. 6. CLEO Monte Carlo spectrum for $B \to \eta X$; (a) from $B \to DX, D \to \eta Y$; (b) from $B \to D_s X, D_s \to \eta Y$; (c) from virtual W^- fragmentation; (d) the sum of (a-c) shown as squares (see text), and the data of Fig. 5 shown as triangles.